Journal of Heat Island Institute International Vol. 12-2 (2017)

Academic Article

Impact of Land Breezes on Nocturnal Temperature in the Osaka Plain

Takashi Ogawa[*1], Ryusuke Yasuda[*1], Atsumasa Yoshida[*1]

[*1] Department of Mechanical Engineering, Osaka Prefecture University

Corresponding author: Ryusuke YASUDA, yasuda@me.osakafu-u.ac.jp

ABSTRACT

To investigate whether land breeze can be effective for the mitigation of nocturnal urban heat island (UHI) in the Osaka Plain, we evaluated land breeze cooling on summer nights. An analysis of observational data shows that there is a mutual relationship between the nocturnal temperature and land breeze. The influence of changes in land use and the sea surface temperature (SST) on long-term trends in nocturnal temperature and land breeze was investigated using a numerical model. The results showed that the effect of land use change was larger than that of SST change. The cooling effect of the nocturnal wind was also evaluated using the change rate of potential temperature by advection. The result indicated that the cooling effect at night was about -0.2 K/h in the Osaka Plain under the sea breeze condition. However, under the land breeze condition, the cooling effect was about -1.0 K/h in inland areas and about -0.6 K/h in the coastal areas. Although the cooling effect of land breezes reduces from inland to the coast, the effect still exists around coastal areas. Therefore the study concluded that land breeze cooling is effective in the mitigation of nocturnal UHI over the entire Osaka Plain.

Key Words : Urban heat island, Land breeze, Temperature, Cooling rate, Advection, Numerical model

1. Introduction

Osaka is the most populous metropolitan area in western Japan and is well known for its severe summertime thermal environment(1). The Osaka Plain is the central area of the Osaka Prefecture, and is surrounded by mountains to the north, east, and south. The western side faces the Osaka Bay (Fig.1). Since land-sea breeze circulations often develop in this area, utilization of the sea breezes is expected to be effective for the mitigation of the daytime urban heat island (UHI) in summer(2)-(4). However, it is well known that UHI is usually remarkable at night(5)(6). High temperatures on summer nights not only deteriorate thermal comfort and increase power consumption by air conditioning units but also lead to increase of sleep disorder and heat stroke(7)(8). To consider using land breezes as measures of nocturnal UHI, it is necessary to investigate the influence of land breeze on the nocturnal temperature and to evaluate its cooling effect.

Cooling effects of sea breezes in the daytime in the Osaka Plain had been investigated by several researchers(9)-(11). On the other hand, research focused on a cooling effect of nocturnal land breezes in the plain are quite a few. In this study, we use the term

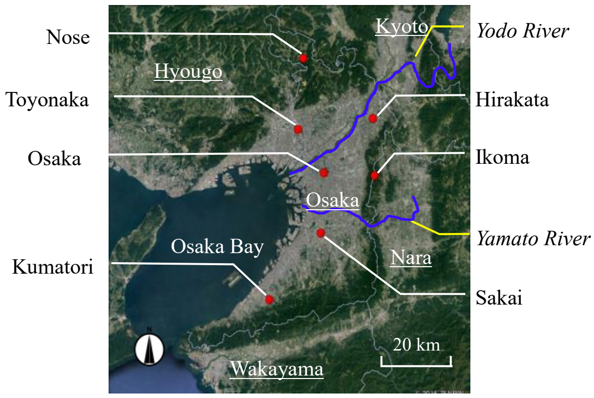

Fig.1 Analysis area. Red filled circles are AMeDAS observation points. Prefecture names are underlined. The photo was obtaned from Google Earth.

"land breeze" as a flow which generates inland and reaches to the coast. Driving force of it is basically a pressure gradient between land and sea, but drainage flow develops in the mountainous areas, which is a density flow, is also included as a source of it.

Characteristic of the land breeze cooling will not be the same as that of sea breeze. Since sea breezes in the daytime advance into a mixing layer, a strong updraft usually accompanies at the leading edge of it. On the other hand, land breezes penetrate into stable layers; therefore, the head has a flattened shape[13] and the updraft at the leading edge is not strong as in the sea breeze. With such a difference, the cooling effect of land breeze might be limited compared to that of sea breeze. Tamai et al.[12] have investigated a cooling effect of nocturnal drainage flows coming from the eastern mountains of the plain. They concluded that the drainage flows do not contribute to the cooling in the central area of the plain; however, the cooling effect of land breezes in the other areas in the Osaka Plain is not clear. In the daytime, the cooling effect of sea breezes become large as the wind speed increases. On the other hand, in the case of the land breeze, high wind speed may lead to an opposite result, in considering that radiative cooling of the ground surface during the nighttime is large under clear and calm conditions. When wind speed of nocturnal land breezes is high, it may obstruct the cooling in surface layer by increasing heat transport from upper warm layer through an enhancement of turbulence mixing.

Another important factor concerned with the land breeze cooling is a trend of its occurrence. According to a report published in 1987 by Osaka Regional Headquarter of Japan Meteorological Agency (JMA)[14], the mean starting time of land breezes was 2300 LST around the center of the Osaka Plain, though the statistical period and the method of the analysis were not shown. Later, Kono et al.[1] also investigated the mean starting time of land breezes in the plain based on observation data obtained on clear days in July from 1994 to 1998. Their results indicated that the mean starting time of the land breeze is late compared to the former study in most of the plain; e.g. the starting time around the center of the Osaka Plain is 0500 LST. They also stated that the nocturnal wind around the coastal area of the Osaka city did not change to land breeze in more than half of the cases. These results may suggest that the land breezes have been weakening in this plain. The reason of such changes is not clear, but it is likely that urbanization in the suburbs of the Osaka city has contributed to the changes. In particular, changes in land use will have a substantial influence on the land-sea breeze circulation of the area through changes in temperature and pressure gradient[15]-[17]. Changes in the sea surface temperature (SST) around the Kansai area may also affect on the land breezes. Tamai et al.[10] pointed out that SST of the Osaka Bay affects the nocturnal temperature in the Osaka Plain. Therefore, nocturnal wind system in the Osaka Plain may be also influenced by the SST. In addition to the cooling effect of the land breeze, the influence of these factors should be investigated.

In this study, we evaluated the land breeze cooling on summer nights in the Osaka Plain to investigate whether utilization of land breezes can be effective for the mitigation of nocturnal UHI. In section 2, we investigated the relationship between nocturnal wind and air temperature on summer nights by an analysis of observational data. In section 3, to investigate whether recent changes in land use and SST affect the land breeze, the influence of these changes were evaluated using a meteorological model. In section 4, the cooling effect of nocturnal land breeze was estimated by numerical simulations. A summary and conclusion are provided in the final section.

2. Relationship between observed nocturnal wind and temperature

The relationship between nocturnal wind and air temperature on summer nights in the Osaka Plain was investigated using a cluster analysis[18] based on hourly observational data obtained from the Automated Meteorological Data Acquisition System (AMeDAS) operated by JMA. The analysis period was in July and August from 2006 to 2009. To avoid the influence of synoptic flow of the wind and precipitation on the temperature, windy days ($|U_g|\geq 15$ m/s) and/or rainy days ($R\geq 1$ mm) were excluded from the analysis, where U_g is the mean geostrophic wind and R is the total precipitation, during 0100-0600 LST at the Osaka meteorological observatory. The geostrophic winds at the point were estimated from the quadratic polynomial fitting of sea surface pressures[19] based on observational data at 27 meteorological observation sites around the Kansai area. The wind speed of 15 m/s is large; however, the surface wind is much smaller than this. Under this condition, the maximum value of mean nocturnal wind (0100-0600 LST) at AMeDAS Osaka site was 5.3 m/s, and 94% were less than 3 m/s.

As a result, data used in this analysis covered 202 days. A degree of distribution similarity (“distance”) between one day (a) and another day (b) for wind, D_{ab}^{W}, was defined as

$$D_{ab}^{W}=\frac{1}{NM}\sum_{i=1}^{M}\sum_{k=1}^{N}\sqrt{(U_{aik}-U_{bik})^2+(V_{aik}-V_{bik})^2} \quad (1)$$

and for temperature, D_{ab}^{T}, as

$$D_{ab}^{T}=\frac{1}{NM}\sum_{i=1}^{M}\sum_{k=1}^{N}\sqrt{(T_{aik}-T_{bik})^2} \quad (2)$$

where U_{aik}, V_{aik}, and T_{aik} are eastward and northward components of hourly wind speed, and air temperature, respectively. The subscript i is the hour, a is the date, and k is the observation point index. N(=7) is the total number of observation points (Fig.1), and M(=6) is average time (0100-0600 LST). The Ward’s method was used as the linkage criterion. We grouped the analysis days into three clusters for the wind (W1–W3) and three clusters for temperature (T1–T3).

Mean wind vectors and air temperatures in each wind cluster during the averaging time at AMeDAS monitoring points are shown in Fig. 2 (W1)-(W3). In W1, the wind direction in the central area of the Osaka Plain is westerly, i.e. this cluster corresponds to a sea breeze pattern. Conversely, in W3 an easterly

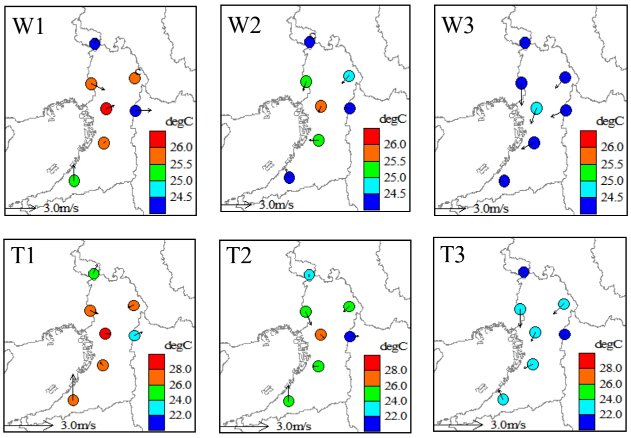

Fig.2 Mean wind vectors and air temperatures in each cluster at AMeDAS monitoring points. W1-W3 (upper) are the wind pattern groups, and T1-T3 (lower) are the temperature pattern groups. All values were averaged from 0100 to 0600 LST.

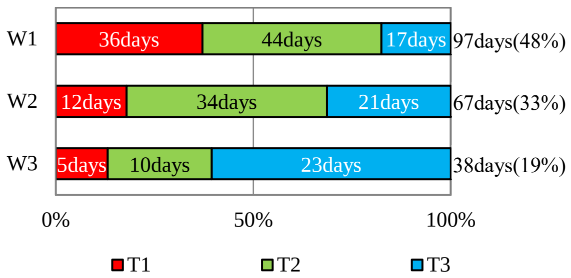

Fig.3 The number of days and percentages in each cross-category between wind and temperature groups.

wind dominates in the area, which indicates this cluster corresponds to a land breeze pattern. The wind direction in W2 is similar to the land breeze pattern; however, the wind speed is relatively weak. Therefore, W2 is regarded as an intermediate pattern between W1 and W2. The frequency of land breeze pattern (W3, 19%) seems to be somewhat too much if the average starting time of the land breezes around the center of the Osaka Plain is 0500 LST as reported by Kono et al.[(1)]; however it is difficult to make further discussions on it quantitatively because detailed conditions of their analyses are not presented. The figures clearly show that mean nocturnal temperature at the monitoring points under the land breeze condition is lower than that under the sea breeze condition. At the AMeDAS Osaka monitoring point, the mean nocturnal temperatures in W1, W2, and W3 are 26.9 °C, 26.0 °C, and 24.8 °C, respectively. In W3, temperatures at other observation points were also 1.2–2.3 °C lower than those in W1.

Fig. 2 (T1)-(T3) show mean nocturnal wind vectors and temperatures averaged in each air temperature cluster. The mean temperature is high in cluster T1 and low in cluster T3. The distribution pattern of mean wind direction in T1 is similar to W1 (sea breeze pattern), and that of T3 is similar to W3 (land breeze pattern).

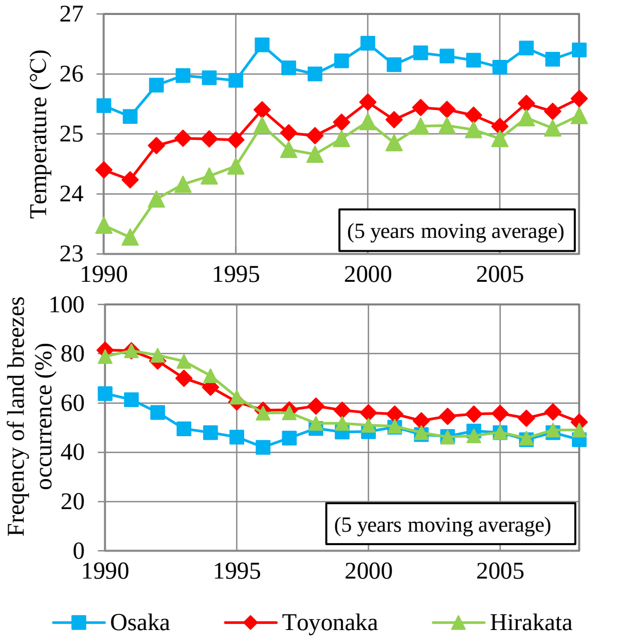

Fig.4 Long-term trends of (a) mean nocturnal temperature and (b) frequency of land breeze occurrence.

The number of days in each cross-category between wind and temperature is shown in Fig.3. In W1, the ratio of T1 is higher than T3, while in W3, the opposite is true. Therefore, nocturnal temperatures in the Osaka Plain are often high under the sea breeze pattern and often low under the land breeze pattern. Although these results do not indicate a cause-effect relationship between the land-sea breeze condition and temperature distribution in the plain during summer nights, they clearly show a mutual relationship between them.

To examine long-term trends in nocturnal land breezes and temperature in the plain, AMeDAS observation data at three points (Osaka, Toyonaka, and Hirakata) were investigated. The analysis period was in July and August from 1988 to 2010. As with the cluster analysis, hourly data during 0100-0600 LST were used and windy/rainy days were excluded. Fig. 4(a) shows long-term changes of mean nocturnal temperature. Nocturnal temperature has been rising at every point. The rates of temperature rise are greater in the early 1990s than later in the study period. Fig. 4(b) shows the trends in land breeze occurrence. The land breeze occurrence was determined from the vector mean of wind directions during 0100–0600 LST at each AMeDAS point. The land breeze directions of the nocturnal wind were identified as the following (clockwise):

- Osaka - N, NNE-ENE
- Toyonaka - NNE-E, NW-N
- Hirakata - NE-SE

with reference to the wind rose at each point. The land breeze ratio

Table 1 Correlation between nocturnal temperature and frequency of land breeze occurrence.

AMeDAS points	Correlation coefficients
Osaka	-0.73 ($p<0.01$)
Toyonaka	-0.68 ($p<0.01$)
Hirakata	-0.63 ($p<0.01$)

decreased over time at every point. Table 1 shows that there are negative correlations between the frequencies of land breeze occurrence and temperatures.

3. Influence of changes in land use and SST on nocturnal land breeze and temperature

3.1 Numerical model

We investigated the influences of land use change in the Osaka area and SST change around the Kansai area on long-term changes in the nocturnal land breeze and temperature using a numerical model; the Weather Research and Forecasting (WRF) modeling system ver.3.7.1[20]. The model parameters are shown in Table 2. Initial and boundary conditions for the meteorological variables were obtained from the Final Operational Global Analysis database of the National Centers for Environmental Prediction, with 1° resolution and 6-hour interval. Grid data of the altitude (50 m resolution) and land use (100 m resolution) were from the National Land Numerical Information database of the National and Regional Planning Bureau. A single-layer urban canopy model[21] was activated on the urban grids specified by the land use data. Anthropogenic sensible heat estimated by Shimoda et al.[22] was given in Domain 2.

The calculation domain is shown in Fig. 5. Two domains were set with a two-way nesting configuration. The depth of the lowest layer was approximately 57 m. A target date of August 26, 2006, was chosen from W3 (land breeze pattern) described in section 2. Calculation started at 0900 LST on August 24, 2006. After the 39 hours spin-up, hourly data of 0100–0600 LST in Domain 2 were

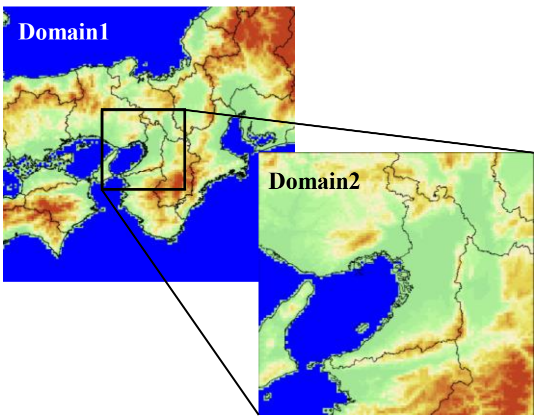

Fig.5 Calculation domains of the numerical model.

Table 2 Calculation parameters of the numerical model.

Items	Domain 1	Domain 2
Horizontal grid interval	3 km	1 km
Number of horizontal grids	120×120	103×103
Central coordinate (Lat.,Long.)	(34.672° ,135.480°)	
Number of vertical layers	30	
Microphysics	WSM-3 Class	
Planetary boundary layer	MYNN Level 2.5	
Surface layer	M-O Similarity Theory	
Longwave radiation	RRTM scheme	
Shortwave radiation	Dudhia scheme	
Land surface model	Noah LSM	
Urban surface model	Single Layer UCM	

used for analysis.

3.2 Analysis cases

The urban ratio in 1976 in Domain 2 is shown in Fig. 6(a). The urban ratio of each calculation grid (1 km square) was defined as a ratio of land use meshes categorized as artificial surfaces (i.e. buildings, major roads, and railways) to the total meshes, based on 100 m land use data. The central area of the Osaka Plain had already urbanized in the mid-1970s and the urban area has been expanding to its suburbs since then. Fig. 6(b) shows the increment of the urban ratio from 1976 to 2009. During this period, the urban ratio clearly increased in the northern and southern edges of the plain, along with the Yodo River, Nara Basin, and coastal areas in Hyogo and Wakayama.

Fig. 7 shows the long-term trend of the SST in summer (July-September) around the whole calculation domain (Domain 1), based on data provided by JMA. SST_N is the SST on the north side of the domain (southwest zone of Sea of Japan) and SST_S is on the south side (off coast zone of Shikoku-Tokai). In the last three decades, they both increase ($p<0.01$) and the rates are approximately +0.02 °C/year.

We simulated three cases as shown below:

- Case1: Baseline. Land use data in 2009 was used.
- Case2: Same as Case 1 but land use was changed to as of 1976.
- Case3: Same as Case 1 but SST was 0.5 °C lower.

3.3 Results and discussions

Fig. 8(a) shows the horizontal distribution of mean nocturnal temperature at 2 m and wind vectors at 10 m (averaged from 0100 to 0600 LST). Two major courses of land breezes can be seen in the Osaka Plain. In the northern portion of the plain, the land breeze flows from the northeast to the southwest along the Yodo River. In the mid-south portion of the plain, the land breeze is generated in the Nara basin, flows through a valley, and proceeds to the west along the Yamato River. The air temperatures along these land breeze pathways are lower than the other areas on the plain. In the central area of the plain (sandwiched between these paths), the land breeze is weak and the temperature is high. Fig. 8(b) shows the differences in mean nocturnal temperatures and wind vectors (0100-0600 LST) between Case 1 and Case 2. Note that the difference between Case 2 and Case1 is brought by a change in the land use only. The calculation result of Case 2 does not represent a meteorological state in 1976 because the calculation conditions other than the land use are the same as 2006. In most of the parts of the plain, from 1976 to 2009, the temperature increased when land use changed. In areas where there is a substantial rise in temperature, there is also a significant increase of urban ratio. The distribution of rising temperatures appears to affect the wind pattern through a change in the pressure gradient. The direction of the difference vectors along the Yodo River is northeast, which indicates that land breeze weakens. Such a change in direction is also true of the area along the Yamato River; the direction of the difference vectors in this area is eastward. Fig. 8(c) shows the differences of nocturnal average temperatures and wind vectors between Case 1 and Case 3. Since the SST in Case 1 is 0.5 °C higher than Case 3, the temperature rise is greater in sea areas but the temperature changes on the land are very small compared to sea areas. The change in the land breezes

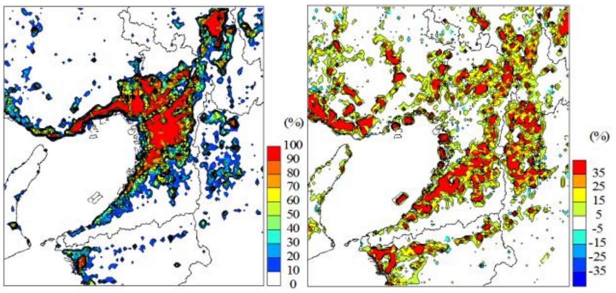

Fig. 6 Distribution of urban ratio (a) in 1976, and (b) its increment from 1976 to 2009.

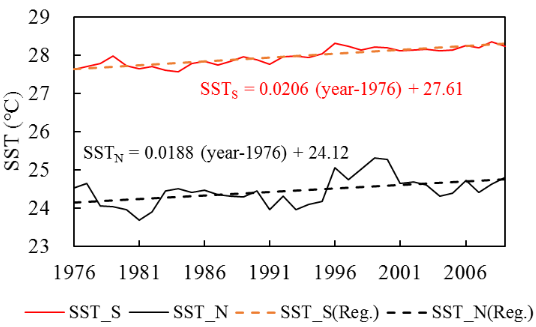

Fig. 7 Changes of mean SST in summer (July-September) from 1976 to 2009. SST_N is "southwest zone of Sea of Japan", and SST_S is "off coast zone of Shikoku-Tokai", according to JMA labeling. Solid line: moving average for 5 years. Dashed line: linear regression.

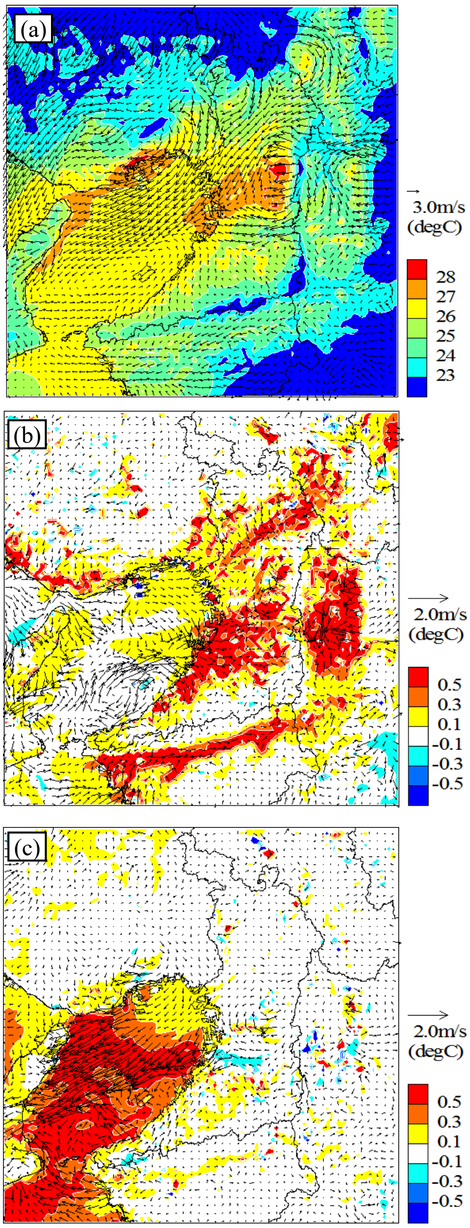

Fig. 8 Horizontal distribution of mean nocturnal temperature at 2 m and wind vectors at 10 m. (a) Distribution on August 26, 2006. (b) Case 1-Case 2, (c) Case 1-Case 3. All of the values were averaged from 0100 to 0600 LST.

in the plain is also small though the land breeze is slightly weakened around the Yodo River and is slightly strengthened around the Yamato River.

Table 3 and Table 4 show the increase of mean nocturnal temperature and the decrease of mean nocturnal wind speed, respectively. These values were obtained by averaging the grid values lower than 100 m in each region shown in Fig. 9. The influence of the changes in SST on the nocturnal temperature and land breezes are very small compared to those of the land use change. As will be shown in section 4.2, the temperature difference between observed and model values at night may reach around 1 °C; however, such value is a measure of the agreement between observation and model values, and it does not directly relate to the sensitivity on the physical mechanisms. These results indicate that the land use change of urbanization has a larger impact on the temperature rise and the land breeze weakening than the SST change.

4. Evaluation of land breeze cooling

4.1 Target cases and evaluation method

To evaluate the land breeze cooling, numerical simulations on the sea breeze case (August 11, 12, and 22, 2006) and land breeze case (August 23, 24, and 26, 2006) were executed using WRF. These days were selected from W1 (sea breeze) and W3 (land breeze) described in section 2, as they are typical conditions of each nocturnal wind pattern. A local cooling effect was evaluated by the change rate of potential temperature. The change rate by each term in the conservation equation for potential temperature is given by

$$\text{Advection:}\quad \left(\frac{\partial\theta}{\partial t}\right)_{adv} = -\frac{\partial(U_j\theta)}{\partial x_j} \tag{3}$$

$$\text{Diffusion:}\quad \left(\frac{\partial\theta}{\partial t}\right)_{diff} = \frac{\partial}{\partial x_j}\left(D_{j\theta}\frac{\partial\theta}{\partial x_j}\right) \tag{4}$$

$$\text{Radiation:}\quad \left(\frac{\partial\theta}{\partial t}\right)_{rad} = \frac{\theta}{T}\frac{1}{\rho C_p}\frac{\partial F}{\partial z} \tag{5}$$

$$\text{Total:}\ \left(\frac{\partial\theta}{\partial t}\right)_{tot} = \left(\frac{\partial\theta}{\partial t}\right)_{adv} + \left(\frac{\partial\theta}{\partial t}\right)_{diff} + \left(\frac{\partial\theta}{\partial t}\right)_{rad} \tag{6}$$

where U_j is a component of wind speed, θ is the potential temperature, T is the air temperature, ρ is the density, C_p is the specific heat at constant pressure, $D_{j\theta}$ is the turbulent diffusion coefficient for heat, and F is the long/short radiation flux. Sensible heat flux from the land and sea surfaces are evaluated in the diffusion term. The values in Eqs. (3) - (5) are evaluated at the lowest grid of the atmospheric layer. The representative height is the midpoint of the 1st layer (ca. 30 m). These terms are calculated by reconstructing the discrete equations of WRF model (including higher order upwind scheme) using grid values extracted from the output file of WRF model. The heat exchange by condensation or evaporation

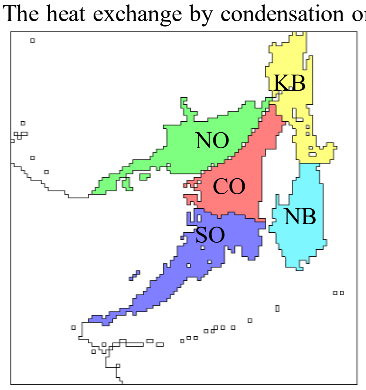

Fig. 9 Averaging regions used in Section 3.3. Altitude is less than 100 m. NO: Northern Osaka, CO: Central Osaka, SO: Southern Osaka, KB: Kyoto Basin, NB: Nara Basin. In NO, a part of Hyogo Prefecture is included.

Table 3 Difference of mean nocturnal temperature averaged in each region (°C).

Factor	Central Osaka	Northern Osaka	Southern Osaka	Kyoto Basin	Nara Basin
Land use (Case1-Case2)	+0.41	+0.33	+0.60	+0.30	+0.85
SST (Case1-Case3)	+0.02	+0.03	+0.07	+0.02	+0.02

Table 4 Difference of mean nocturnal wind speed averaged in each region (m/s).

Factor	Central Osaka	Northern Osaka	Southern Osaka	Kyoto Basin	Nara Basin
Land use (Case1-Case2)	-0.24	-0.25	-0.28	-0.18	-0.43
SST (Case1-Case3)	-0.15	-0.13	-0.22	-0.07	-0.16

was not included. The spin-up time was 39 hours before the target days and hourly data of 0100–0600 LST in Domain 2 were used for analysis (same as Section 3).

4.2 Results and discussions

4.2.1 Comparison of the model results with observations

Statistical evaluations were made using the measurements of the surface monitoring stations in the Osaka Prefecture (9 AMeDAS sites and 59 meteorological monitoring stations operated by local governments). The statistics are defined as follows:

Mean Bias Error (MBE)

$$MBE = \bar{M} - \bar{O} \tag{7}$$

Mean Gross Error (MGE)

$$MGE = \overline{|M - O|} \tag{8}$$

Root Mean Square Error (RMSE)

$$RMSE = \{\overline{|M - O|^2}\}^{\frac{1}{2}} \tag{9}$$

Index of Agreement (IA)

$$IA = 1 - \frac{\overline{(M - O)^2}}{\overline{(|M - \bar{O}| + |O - \bar{O}|)^2}} \tag{10}$$

where O represents the surface measurements and M represents model values (wind speed at 10 m or air temperature at 2 m) at the monitoring points. Both are hourly values. The overline indicates the arithmetic mean of all hours for all points. Table 5 shows the results and the benchmarks recommended by Emery et al.[23] The boundary of a day is 0900 LST and the label is the date of the last hour. All of the MGE and IA values of temperature and the RMSE of wind speed are within the recommended values, though the MBEs indicate that the model tends to over predict the wind speed

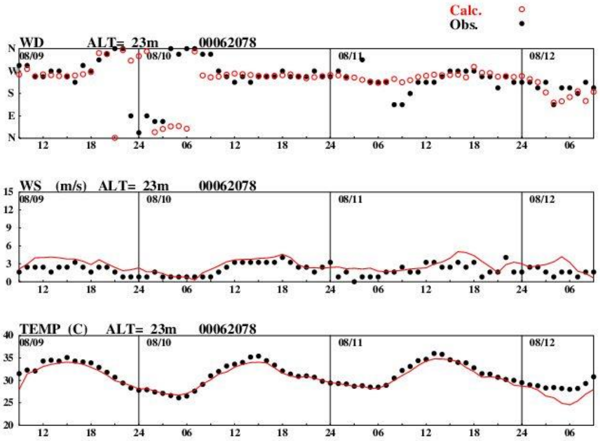

(a) August 11,12, 2006

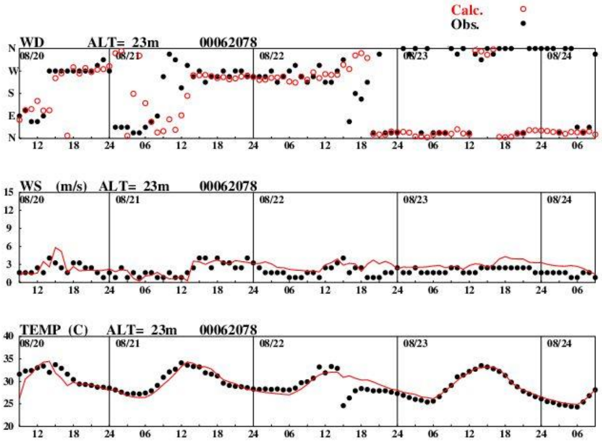

(b) August 22-24, 2006

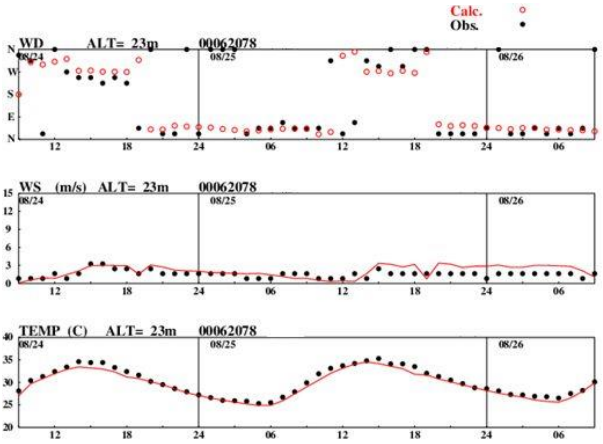

(c) August 24, 26, 2006

Fig. 10 Comparison between observed value and calculation result at Osaka AMeDAS point. Observed wind speeds were adjusted to a value at 10 m above ground level using a Log law. Period of (a)-(c) was calculated individually. First 39 hours in each run is spin-up period.

and under predict the air temperature. As shown in Fig. 10, the agreement between the model result and the observations is fairly good. The model results successfully reproduced the changes in temperature and wind except for a shower in the late afternoon on August 22.

The nocturnal flows would be shallow under the stable conditions, and the locality of the flows might be prominent compared with those in the daytime. To investigate whether WRF performance degrades at night, the evaluation indices shown above were estimated for each time zone (01-06, 07-12, 13-18, 19-24 LST) during the analysis period.

Fig.11 shows the result of temperature indices. In general, IA value in each time zone is smaller than the daily value because the variation during an averaging time is included in the denominator of the fraction in IA. Note that the difference from the observations was particularly large in the daytime on 22 August (22D) because of an occurrence of the shower which was not predicted by the model. The MBEs of temperature sometimes show large positive or negative values and exceed the range recommended by Emery et al.[23] especially in the morning (yellow bars) and daytime (red bars). Time series comparison between the observation and model results suggests that high temperatures in the daytime tend to be predicted somewhat lower. The nighttime values of MBE (black bars) except 12 August (12N) are generally smaller than those in the morning and daytime. All of MGEs except 22D are within the recommended range. Since variations of temperature in the nighttime are smaller than those in the daytime, MGEs in the nighttime often show small values in comparison with the daytime values. IAs in the nighttime except 12 August satisfy the benchmark value.

Fig.12 shows the variation of the evaluation indices on wind speed. The MBEs show that the wind speeds are overpredicted in most of the time zones, especially in the evening and nighttime. As of 2006, wind speeds at AMeDAS points were recorded in 1 m/s unit, therefore the MBE's benchmark of 0.5 m/s might be too restrictive. All of the RMSEs are within the recommended range, but it must be taken into account that the wind speed is generally small at night, which leads to a small value of RMSE. IAs of wind speed for each time zone in the daytime seems to show relatively large values in comparison with the nighttime though only a few of them satisfy the benchmark.

Table 5 Evaluation indices of agreement between calculation and observation. Boldfaces indicate within the benchmarks.

Date	Air temperature			Wind speed		
	MBE (°C)	MGE (°C)	IA	MBE (m/s)	RMSE (m/s)	IA
	≦±0.5	≦2.0	≧0.8	≦±0.5	≦2.0	≧0.6
2006/8/11	**-0.20**	**1.00**	**0.94**	0.98	**1.34**	**0.66**
2006/8/12	-1.05	**1.35**	**0.93**	1.03	**1.69**	0.49
2006/8/22	-0.70	**1.00**	**0.94**	0.64	**1.29**	0.59
2006/8/23	**0.35**	**1.25**	**0.87**	0.80	**1.56**	0.51
2006/8/24	**-0.41**	**0.90**	**0.97**	0.88	**1.46**	**0.62**
2006/8/26	-0.76	**1.43**	**0.92**	**0.30**	**1.11**	0.54

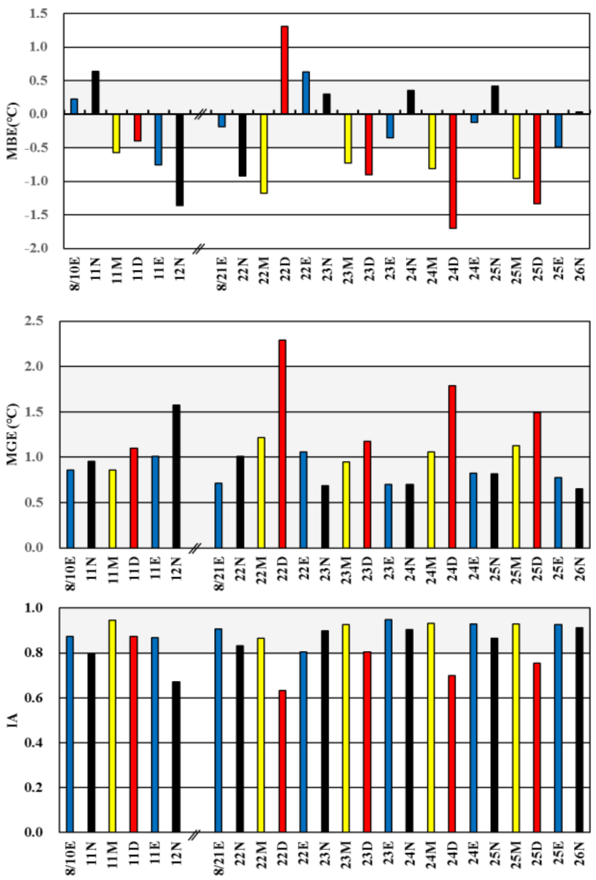

Fig.11 Evaluation indices about temperature in every time zone during the analysis period. Upper: MBE, Middle: MGE, Lower: IA. The horizontal axis indicates a date (in August, 2006) with time zone suffix. The suffixes are N:nighttime (01-06 LST, Black bars), M:morning (07-12 LST, yellow bars), D: daytime (13-18 LST, Red bars) and E:evening(19-24 LST, Blue bars). Gray areas show the ranges recommended by Emery et al.[23]

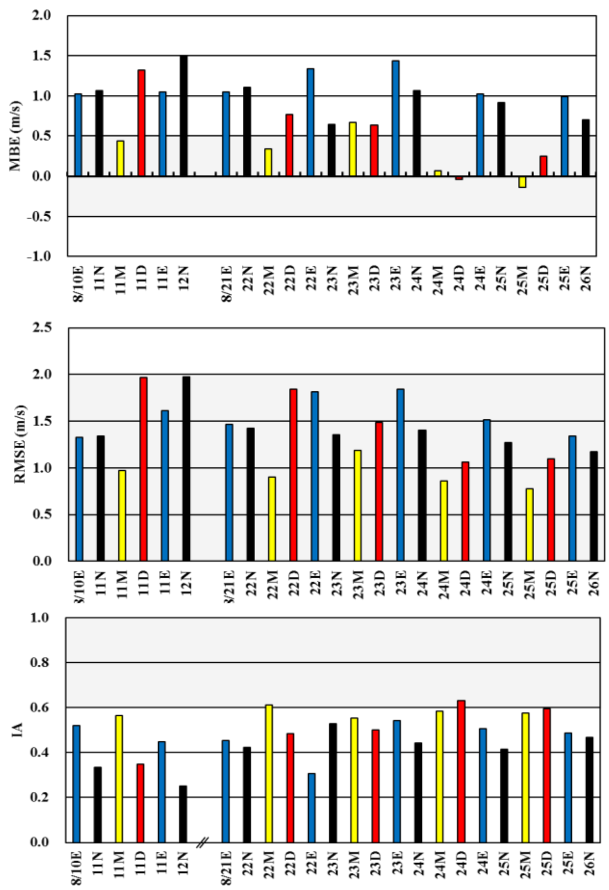

Fig.12 Evaluation indices about wind speed in every time zone during the analysis period. Upper: MBE, Middle: RMSE, Lower: IA. The horizontal axis is the same in Fig.11.

These results suggest that the WRF accuracy in the nighttime is not so inferior to that in the daytime, at least from the point of view of the evaluation indices we have used.

4.2.2 Mean distribution of nocturnal wind and temperature

Model results were averaged in each case to reduce the fluctuation brought by the day-to-day disturbance. The distribution of mean temperature and wind vectors averaged in 0100-0600 LST is shown in Fig. 13(a)(b). During the night in the sea breeze case, the air temperature is high in the central and northern areas of the Osaka Plain because the sea breezes with high temperature keep proceeding over the plain along the Yodo River. A remarkably high-temperature region is located inland along the Yodo River because the cooling effect of the sea breeze is weakening at the location. Mean temperature and wind vectors in the land breeze case show almost the same distributions as Fig. 8(b) in Section 3 (which is also a land breeze case). Compared to the sea breeze case, the temperature along the Yodo River and the Yamato River, the main routes of the land breeze, are relatively low and a high-temperature region appears in the eastern part of the plain.

4.2.3 Cooling effect of nocturnal flow

Fig. 14(a)(b) shows the time series of the change rates of each term in the conservation equation of potential temperature in the lowest layer of a grid where an Osaka AMeDAS site is present. As pointed out by Yoshida et al.[4], in both cases, the variation in the change rate of the advection term is almost the same in magnitude but opposite in sign to that of diffusion term. In the sea breeze case, cooling by advection in the daytime is significant, but it becomes much less at night. The daytime cooling by advection in the land breeze case is less than the sea breeze case, but it does not reach the low cooling levels at night shown in the sea breeze case. Note that the wind during the day is sometimes sea breeze in the land breeze case because both cases are categorized by wind direction only at night. The cooling rate by advection at night is -0.3 K/h approximately in the sea breeze case and approximately -1.0 K/h in the land breeze case. The diffusion heating during the nighttime

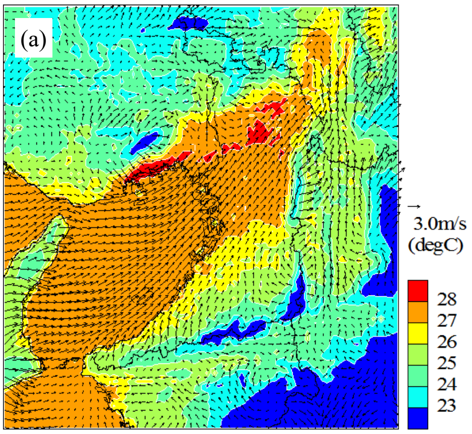

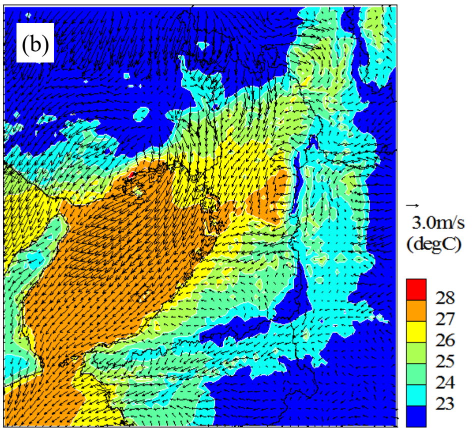

Fig. 13 Distribution of mean nocturnal temperature at 2 m and wind vectors at 10 m (a) in the sea breeze case, (b) in the land breeze case. Averaged values from 0100 to 0600 LST on all days in each case are shown.

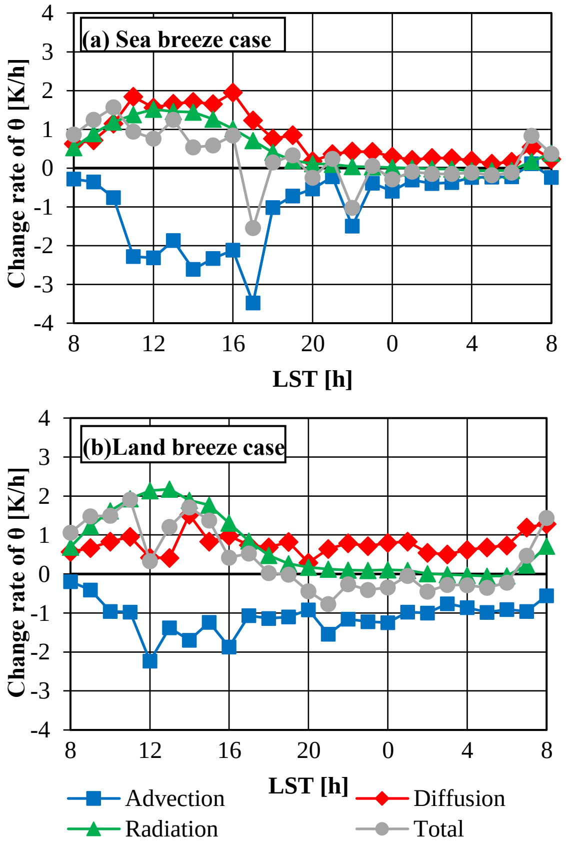

Fig.14 Change rates of each term in the conservation equation of potential temperature at Osaka AMeDAS point (the lowest layer). (a) the sea breeze case. (b) the land breeze case. Averaged values of all days in each case .

in the land breeze case is greater than in the sea breeze case. This is because the air temperature in the land breeze is lower than that of the temperature in the sea breeze and there is a large temperature difference between the ground surface and the air. In the sea breeze case, sea breeze at high temperatures continue to flow at night, and the temperature remains high. On the other hand, in the land breeze case, colder wind flows from surrounding mountainous and/or rural areas remove heat from the urban surface. In an urban area, heat flux at the ground surface is often positive even at night[24]. Heat transport to the upper layer at the top of the lowest layer by turbulent diffusion is smaller than the surface heat flux because net change rate of diffusion term is positive. Radiation term shows negative value at night but small in magnitude. Therefore, the cooling effect of the advection is important, especially in urban area.

Fig. 15(a)(b) shows the horizontal distribution of the cooling rate by advection in the lowest layer of the model over the plain area (altitude is less than 100 m). In the sea breeze case the cooling rate is about -0.2 K/h on the plain. In the land breeze case, the cooling rate is -1.0 K/h approximately in inland areas, and -0.6 K/h approximately in coastal areas. Although the cooling effect of land breezes reduces from inland to coastal areas, the effect remains even around the coasts. In the temperature distributions under the land breeze condition (Fig.8 (a) and Fig.13 (b)), a relatively high-temperature area exists on the eastern side of Osaka Prefecture. In there, cooling rate by advection is also small. These distributions suggest that the drainage flow from Mt. Ikoma seems not to have a direct influence of cooling in this area, as described in Tamai et al.[12]. The cooling of the area and the central area of the Osaka Plain is brought by the land breeze along the main route of the land breeze. Therefore, it is concluded that land breeze cooling is effective in the mitigation of nocturnal UHI over the entire area of the Osaka Plain.

5. **Conclusion**

In the Osaka Plain, the nocturnal temperature and the land-sea breezes have a mutual relationship. The nocturnal temperature is relatively low under the land breeze cases and relatively high under the sea breeze cases. From 1976 to 2009, the nocturnal temperature has increased and the frequency of the land breeze has decreased through the plain. The influence of changes in land use and SST on the trends in the nocturnal temperature and the land

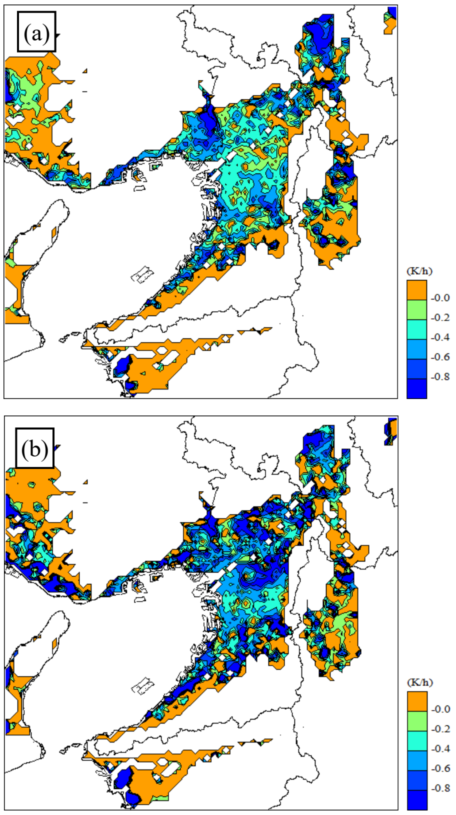

Fig.15 Horizontal distribution of change rates of potential temperature by advection (the lowest layer). (a) the sea breeze case. (b) the land breeze case. Averaged values of all days in each case .

breezes were investigated using a numerical model. The results showed that the effect of land use change was larger than that of SST change. The cooling effect of the nocturnal wind was evaluated using a change rate of potential temperature by advection. The cooling effect of land breezes reduces from inland to coastal areas but remains even around the coasts. Therefore, it is concluded that land breeze cooling is effective in the mitigation of nocturnal UHI over the entire area of the Osaka Plain.

References

(1) H. Kono, D. Narumi, Y. Shimoda, Osaka, Klimaatlas for Urban Environment (in Japanese), Architectural Institute of Japan Ed. (2000), pp.53–65, Gyousei.

(2) City of Osaka, “Kaze-no-Michi” vision [Basic policy], available from <http://www.city.osaka.lg.jp/kankyo/page/0000123906.html> (2011), [March 31, 2017].

(3) Y. Ishii, M. Tamai, K. Muraoka, An Interaction between Heat-island and Sea Breeze in the Osaka Plain (in Japanese), Journal of Japan Society of Fluid Mechanics 19 (2000), pp.139–142.

(4) A. Yoshida, J. Yashiro, X. Xiao, R. Yasuda, Influence of heat Transport by Sea Breezes on Inland Temperature in the Osaka Area, Journal of Heat Island Institute International, 9-2 (2014), pp.6–10.

(5) T.R. Oke, Boundary layer climates (1987), 2nd Ed., Routledge, p.290, New York.

(6) Ministry of the Environment, The guideline of the mitigation for heat island in 2012 (in Japanese), 12–28 [accessed February 17, 2017]http://www.env.go.jp/air/life/heat_island/guidline/h24.html.

(7) Y. Okuno, T. Ihara, Y. Genchi, Evaluation of Environmental Impacts on Disturbed Sleep by Nighttime Urban Heat Island Phenomena using Surveys via the Internet (in Japanese), Journal of Heat Island Institute International, 3 (2008), pp.22–33.

(8) S. Nakai, Number of Deaths from Heat Stroke and Meteorological Condition, -A Survey of the last 21 years in Japan-, Jpn. J. Biometeor., 30-4 (1993), pp.169–177.

(9) H. Takebayashi, M. Moriyama, Urban Heat Island Phenomena Influenced by Sea Breeze, AIJ J. Technol. Des., 21 (2005), pp.199–202.

(10) M. Tamai, T. Arimitsu, Relationship between Nocturnal Temperature and Sea- and Land-Breezes in the Osaka Bay Area in a Summer Season (in Japanese), Environmental Systems Research 36 (2008), pp.397–405.

(11) H. Takebayashi, M. Moriyama, Study on Air Temperature Reduction by Sea Breeze based on Upper Weather Data Analysis, J. Environ. Eng., AIJ, 74-643 (2009), pp.1099–1105.

(12) M. Tamai, S. Ohta, Nocturnal Drainages in the Western Osaka Plain; Their Occurrence Conditions and Relationships with those in the Northern Osaka Plain, J. Japan Soc. Civil Engineers, Ser. G (Environ. Research), 68 (2012), pp.585–593.

(13) S. Mitsumoto, H. Ueda, A Laboratory Experiment on the Dynamics of the Land and Sea Breeze, J. Atmos. Sci, 40 (1983), pp.1228–1240.

(14) Osaka Regional Headquarter of Japan Meteorological Agency, Meteorological phenomena during 100 years in Osaka (“Osaka-no-Kishou 100 Nen”, in Japanese) (1982), pp.36–37, Gyosei.

(15) H. Yoshikado, Vertical Structure of the Sea Breeze penetrating through a Large Urban Complex, J. Appl. Meteor., 29 (1990), pp.878–891.

(16) H. Yoshikado, Numerical Study of the Daytime Urban Effect and Its interaction with the Sea Breeze, J. Appl. Meteor., 31 (1992), pp.1146–1164.

(17) H. Kusaka: The Effects of Land-Use Alternation on the Sea Breeze and Daytime Heat Island in the Tokyo Metropolitan Area, J. Meteor. Soc. Japan, 78-4 (2000), pp.405–420.

(18) Y. Hirano, R. Shibasaki, Classification of the Wind Systems in Kanto Plain by using Cluster Analysis, Proc. Hydraul. Eng., 45 (2001), pp.235–240.

(19) M. Mizuma, General Aspects of Land and Sea Breezes in Osaka Bay and Surrounding Area, J. Meteor. Soc. Japan. Ser. II, 73 (1995), pp.1029–1040.

(20) W.C. Skamarock, J.B. Klemp, J. Dudhia, D.O. Gill, D.M.

Barker, M.G. Duda, X.Y. Huang, Wei Wang, J.G. Powers, A description of the advanced research WRF Ver.3 (2008), NCAR Technical Note.
(21) H. Kusaka: Coupling a single-layer urban canopy model with a simple atmospheric model, Impact on urban heat island simulation for an idealized case, J. Meteor. Soc. Japan, 82-1 (2004), pp.67–80.
(22) Y. Shimoda, Y. Takahara, S. Kametani, D. Narumi, M. Mizuno, Estimation and Evaluation on Energy Flow in Osaka Prefecture, Material and Energy Metabolism in Urban Area and Their Relationships with Buildings Part 2 (in Japanese), J. Archit. Plann. Environ. Eng., AIJ, 555 (2002), pp.99–106.
(23) C. Emery, E. Tai, G.Yarwood, Enhanced meteorological modeling and performance evaluation for two Texas ozone episodes (2001), Project report prepared for the TNRCC, US.
(24) H. Kusaka, F. Kimura, Thermal effects of urban canyon structure on the nocturnal heat island: Numerical experiment using a mesoscale model coupled with an urban canopy model, J. Appl. Meteor., 43 (2004), pp.1899–1910.

(Received Apr. 30, 2017, Accepted Jul. 7, 2017)